Progress in NNLO calculations for scattering processes

Nigel Glover (IPPP, Durham)

September 2002

▷ basic scattering processes like (for example)

- $pp \to$ jets,
- $ep \to 2+1$ jets,
- $e^+e^- \to 3$ jets

where the data is copious (and very precise) at LEP, TEVATRON, HERA, LHC and LC.[a]. Processes with massless internal propagators and at most one off-shell leg.

- Why go beyond NLO?
- Method
- Brief survey of results
- Outlook

[a] Not single scale processes like DIS, Drell-Yan or Higgs production (see later)

Why go beyond NLO?

In many cases, the uncertainty from the pdf's and from the choice of renormalisation scale give uncertainties that are as big or bigger than the experimental errors.

- Measurement of strong coupling constant in $p\bar{p} \rightarrow jet$ by CDF

- Extracting α_s at each value of jet energy demonstrates running of coupling constant and gives

$$\alpha_s(M_Z) = 0.1178 \pm 0.0001(stat)^{+0.0081}_{-0.0095}(exp.syst)$$

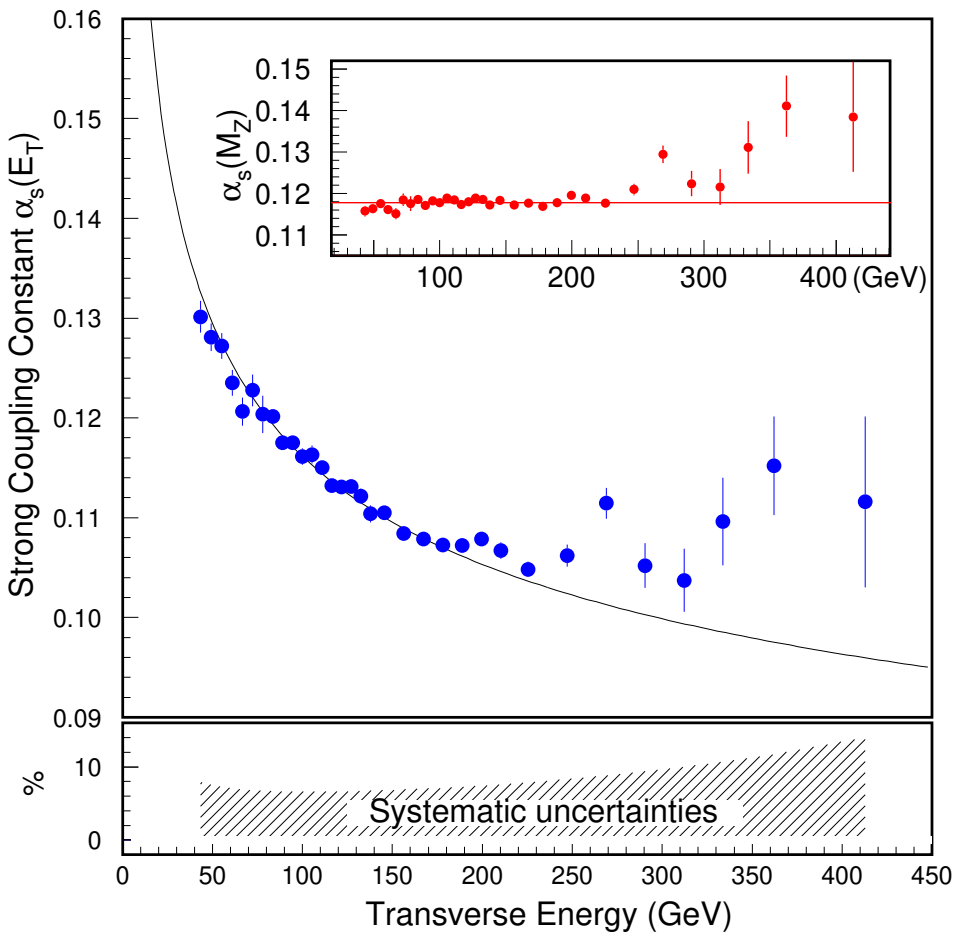

e.g. theoretical uncertainties in α_s extraction from $p\bar{p} \to$ jet are due to renormalisation scale and pdf's

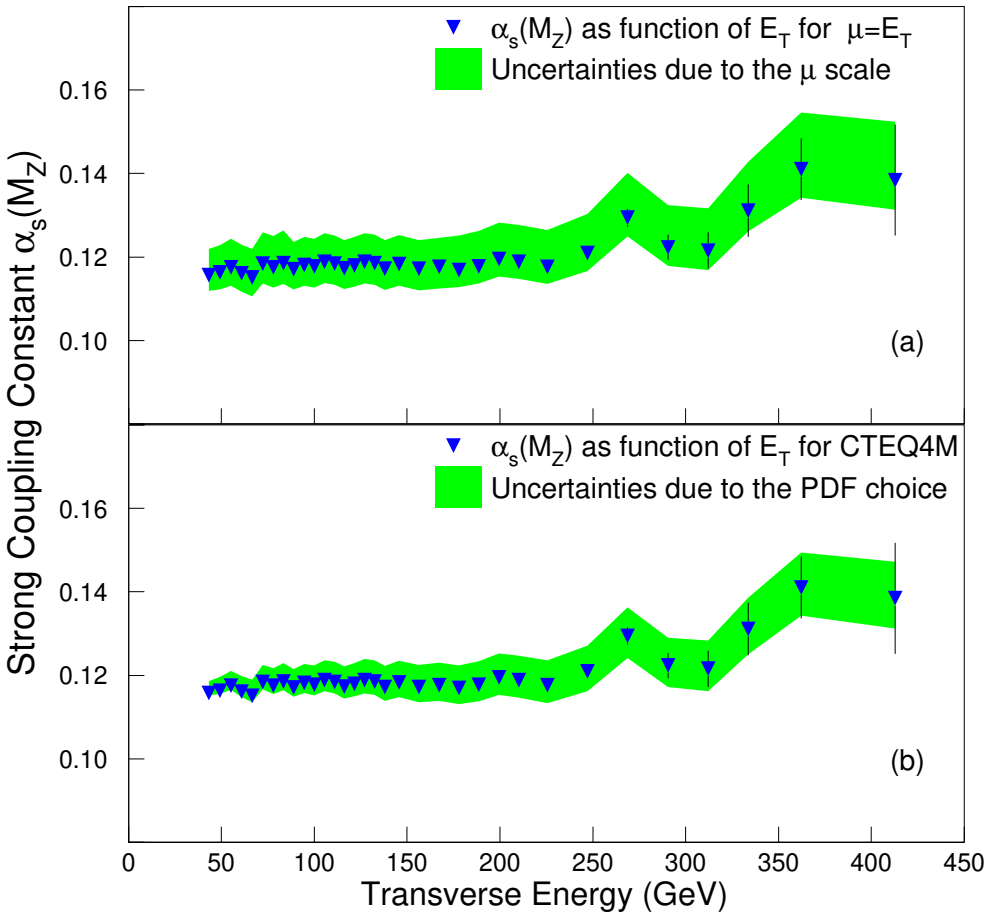

$$\alpha_s(M_Z) = 0.1178 \pm 0.0001(stat)^{+0.0081}_{-0.0095}(exp.syst)$$
$$^{+0.0071}_{-0.0047}(scale) \pm 0.0059(pdf)$$

Why do we vary renormalisation scale?

- The theoretical prediction should be independent of μ_R
- The change due to varying the scale is formally higher order. If an observable $\mathcal{O}bs$ is known to order α_s^N then,

$$\frac{\partial}{\partial \ln(\mu_R^2)} \sum_0^N A_n(\mu_R)\alpha_s^n(\mu_R) = \mathcal{O}\left(\alpha_s^{N+1}\right).$$

- ... but the variation only produces copies of the lower order terms

  e.g.

$$\mathcal{O}bs = A_0\alpha_s(\mu_R) + \left(A_1 + b_0 A_0 \ln\left(\frac{\mu_R^2}{\mu_0^2}\right)\right)\alpha_s(\mu_R)^2$$

  A_1 will contain logarithms and constants that are not present in A_0 and therefore cannot be predicted by varying μ_R.

  For example, A_0 may contain infrared logarithms L up to L^2, while A_1 would contain these logarithms up to L^4.

- μ_R variation is only an estimate of higher order terms
- A large variation probably means that predictable higher order terms are large - but doesnt say anything about A_1.

Renormalisation scale dependence

For example, $p\bar{p} \to$ jet, scale dependence is predictable with NLO calculation

$$\begin{aligned}\frac{d\sigma}{dE_T} &= \alpha_s^2(\mu_R)A \\ &+ \alpha_s^3(\mu_R)\left(B + 2b_0 L A\right) \\ &+ \alpha_s^4(\mu_R)\left(C + 3b_0 L B + (3b_0^2 L^2 + 2b_1 L)A\right)\end{aligned}$$

with $L = \log(\mu_R/E_T)$.

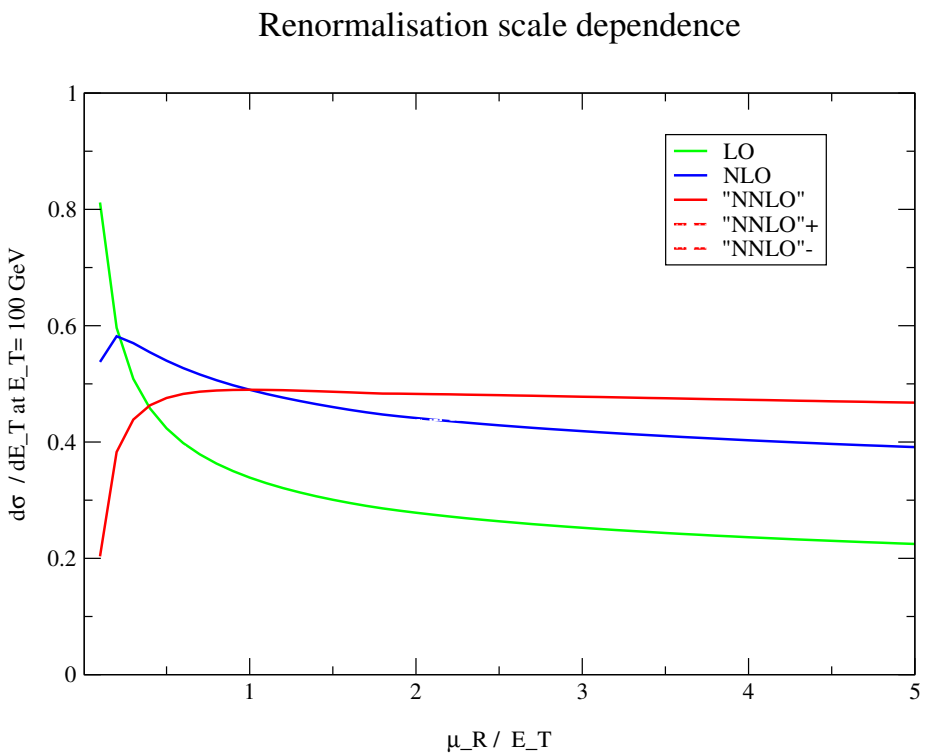

Figure 1: Single jet inclusive distribution at $E_T = 100$ GeV and $0.1 < |\eta| < 0.7$ at $\sqrt{s} = 1800$

The NNLO coefficient C is unknown. The curves show guesses $C = 0$ (solid) and $C = \pm B^2/A$ (dashed). Scale

Renormalisation scale uncertainty

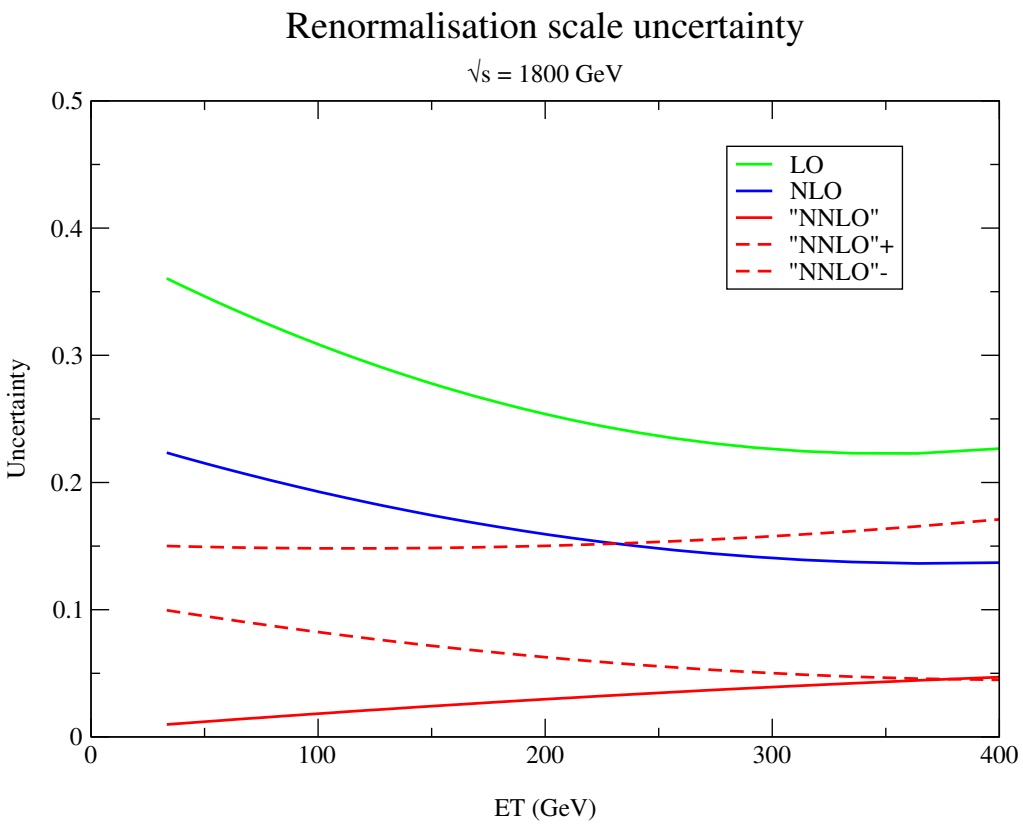

Figure 2: Uncertainty obtained by varying μ_R between $E_T/2$ and $2E_T$ (and keeping $\mu_F = E_T$).

$\Longrightarrow$ Inclusion of NNLO contribution should significantly decrease theoretical renormalisation scale uncertainty for that observable

Jet algorithms

Also there is a mismatch between the number of hadrons and the number of partons in the event. At NLO at most two partons make a jet - while at NNLO three partons can combine to form the jet

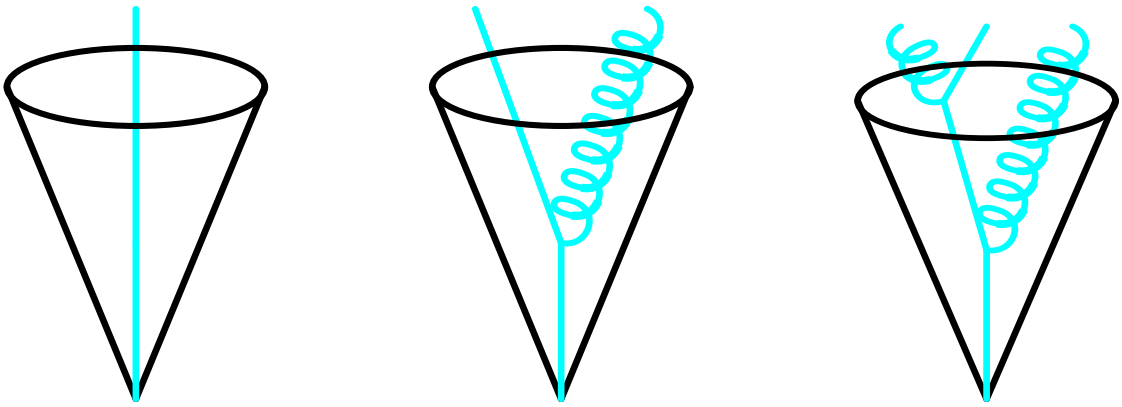

LO NLO NNLO

Perturbation theory starts to reconstruct the shower

$\Longrightarrow$ better matching of jet algorithm between theory and experiment

$\Longrightarrow$ need for better jet algorithms

Description of the initial state

LO At lowest order final state has no transverse momentum

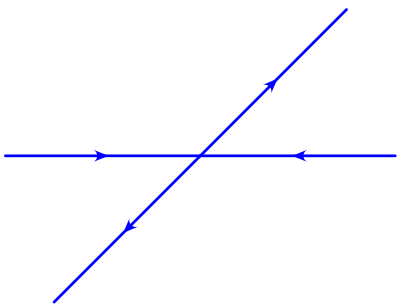

NLO Single hard radiation gives final state transverse momentum, even if no additional jet observed

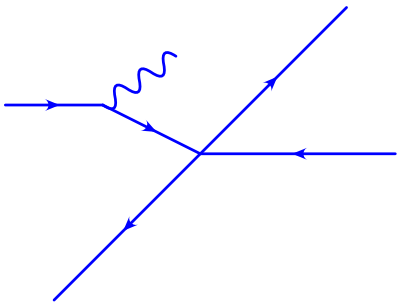

NNLO Double radiation on one side or single radiation off each incoming particle gives more complicated transverse momentum to final state

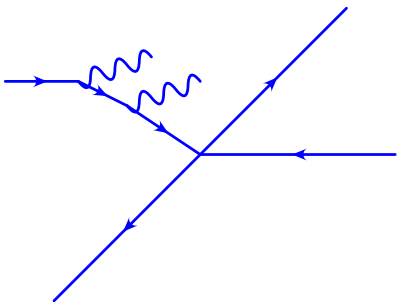

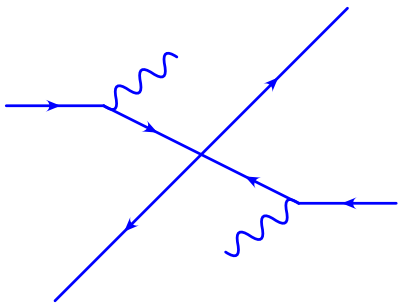

Higher orders and power corrections

NLO Phenomenological power corrections match data with coefficient of $1/Q$ extracted from data.

$$\langle 1-T\rangle \sim 0.33\alpha_s + 1.0\alpha_s^2 + \frac{\lambda}{Q}$$

At NLO, $\lambda \sim 1$ GeV gives a good description of the data.

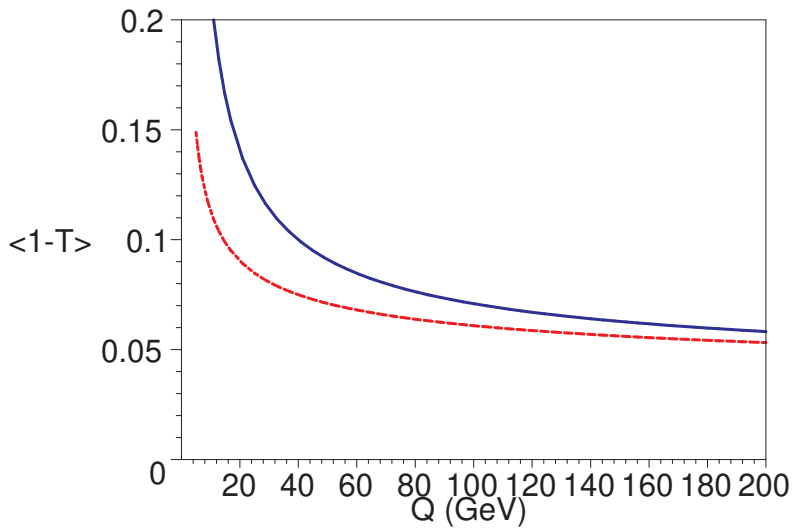

Figure 3: .$\langle 1-T\rangle$ with NLO and no power correction and NLO with power correction $\lambda = 1$ GeV.

The power correction parameterises the unknown higher orders as well as the genuine non-perturbative correction

Higher orders or power corrections

NNLO Higher orders partially remove need for power correction

$$\langle 1 - T \rangle \sim 0.33\alpha_s + 1.0\alpha_s^2 + A\alpha_s^3 + \frac{\lambda \text{ GeV}}{Q}$$

If we guess $A = 3$, then $\lambda = 0.5$ GeV is good fit.

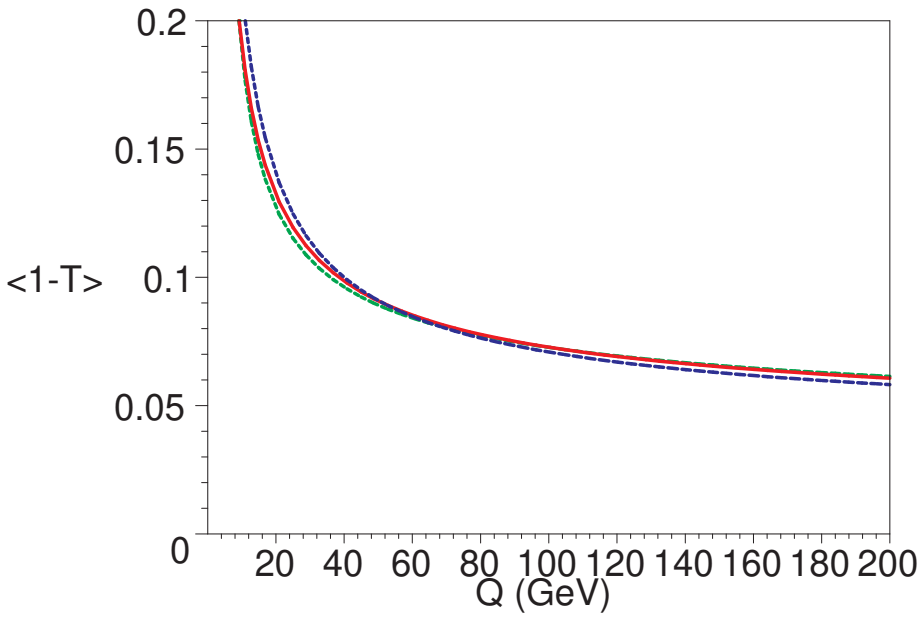

Figure 4: $\langle 1-T \rangle$ with NLO and $\lambda = 1$ GeV, "NNLO" with $\lambda = 0.5$ GeV and "All orders" with no power correction.

At present data not good enough to tell difference between $1/Q$ and $1/\log(Q/\Lambda)^3$.

All orders If higher orders form geometric series, then can avoid power correction altogether!!

Why go beyond NLO? - summary

We expect a variety of improvements at NNLO

- $\surd$ Reduced renormalisation scale dependence
- $\surd$ Better matching of parton-level jet algorithm with experimental hadron-level algorithm
- $\surd$ Better description of transverse momentum of final state due to double radiation of initial state
- $\surd$ Reduced power correction as higher perturbative powers of $1/\ln(Q/\Lambda)$ mimic genuine power corrections like $1/Q$.
- $\surd$ Full NNLO global fit of PDF's should also reduce the theoretical uncertainty
- $\surd$ ...

These improvements will be necessary if and when the experimental accuracy for a given observable is better than the 10% level.

Multiparticle production: NNLO

Example, pure gluon ingredients to $pp \longrightarrow 2$ jets

- 2 loop, 2 parton final state

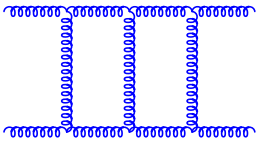

- $|$ 1 loop $|^2$, 2 parton final state

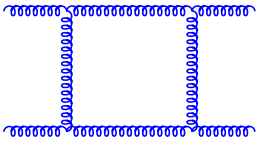

- 1 loop, 3 parton final states
  or 2+1 parton final state

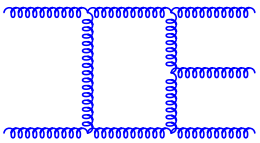

- tree, 4 parton final states
  or 3+1 parton final states
  or 2+2 parton final state

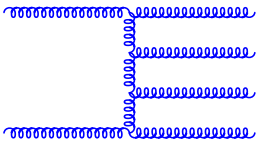

where n theoretically unresolved soft or collinear partons are indicated as +n

▷ Much more sophisticated infrared cancellation between

- n and $n+1$ particle contributions when one particle unresolved
  $\Longrightarrow$ soft and collinear limits of one loop amplitudes
- n and $n+2$ particle contributions when two particles unresolved

▷ For now focus on two-loop contributions.

Two-loop matrix elements for scattering processes

On-shell Process	Tree $\times$ Two-loop	Helicity amplitudes
$e^+e^- \to \mu^+\mu^-(e^+e^-)$	$\surd$(00)	
$q\bar{q} \to q\bar{q}(\bar{q}'q')$	$\surd$(00)	
$q\bar{q} \to gg$	$\surd$(01)	
$gg \to gg$	$\surd$(01)	$\surd$(00), $\overline{\surd}$(02)
$gg \to \gamma\gamma$	—	$\surd$(01)
$\gamma\gamma \to \gamma\gamma$	—	$\surd$(01), $\overline{\surd}$(02)
$q\bar{q} \to g\gamma(\gamma\gamma)$	$\surd$(02)	
Off-shell Process		
$e^+e^- \to q\bar{q}g$	$\surd\surd$(01)	$\surd\surd$(02), $\surd$(02)

$\surd$ Bern, De Freitas, Dixon, Ghinculov, Kosower, Wong

$\surd$ Anastasiou, Binoth, Glover, Marquard, Oleari, Tejeda-Yeomans, van der Bij

$\surd\surd$ Garland, Gehrmann, Glover, Koukoutsakis, Remiddi

$\surd$ Moch, Uwer, Weinzierl

Rapid progress in last two years...

Structure of Two-loop contribution

- The task is to write the many thousands of loop integrals appearing in the amplitude in terms of a few Master Integrals MI_j

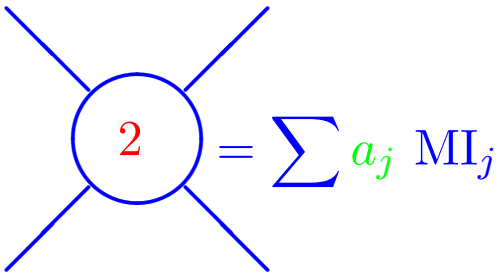

where the a_j are functions of the particle spinors, the kinematic scales and the space-time dimension D. Rewriting Feynman diagrams in terms of the basis set of MI_j is an algebraic task.

Tools
- Integration by parts identities
- Lorentz Invariance identities

- The MI_j need to be expanded in $\epsilon = (4 - D)/2$ so that

$$\mathrm{MI}_j = \sum_{i=1}^{4} \frac{X_i}{\epsilon^i} + X_0$$

Tools
- Mellin-Barnes integral representation
- Differential Equations

On-shell Master Integrals

- The trivial topologies

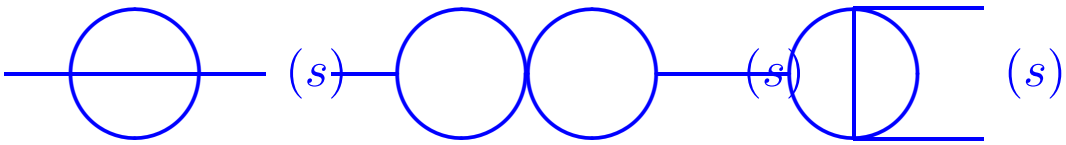

- The less trivial topologies

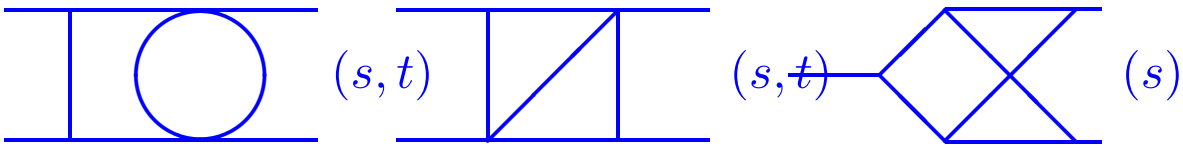

- The non-trivial topologies
  - ▷ The planar boxes

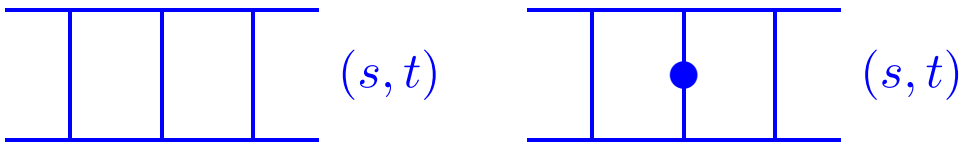

Smirnov, hep-ph/9905323

Smirnov and Veretin, hep-ph/9907385

  - ▷ The non-planar boxes

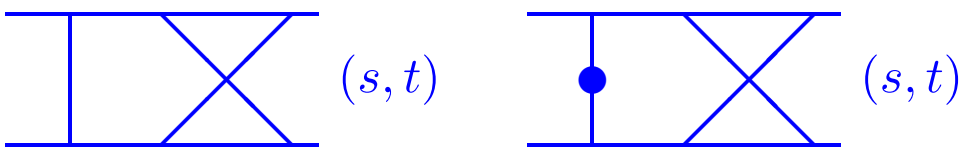

Tausk, hep-ph/9909506

Anastasiou, Gehrmann, Oleari, Remiddi and Tausk, hep-ph/0003261

Two-loop integral inheritance chart

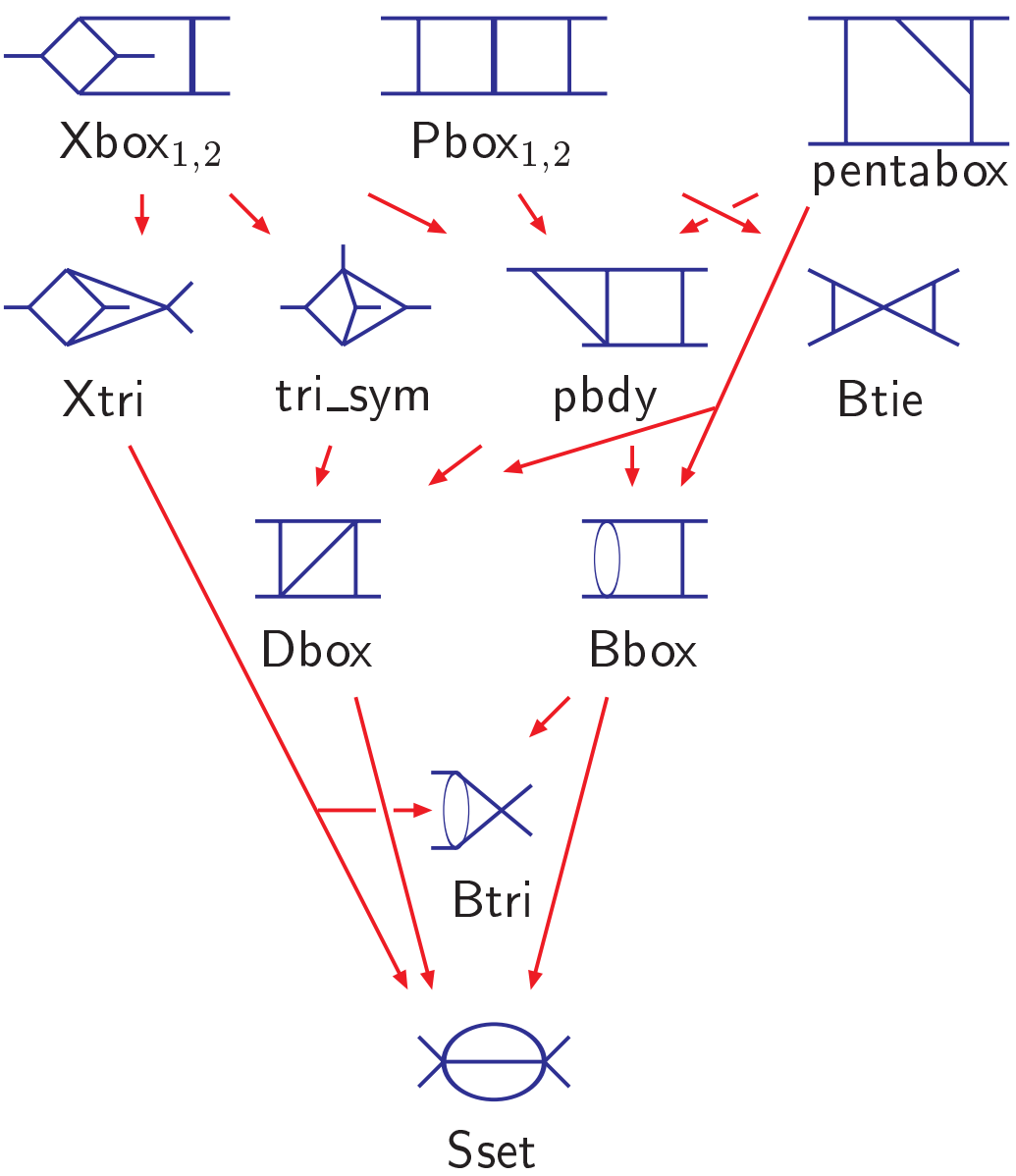

Master Integrals - one offshell leg

- Much more complicated and require new (2-dimensional harmonic polylogarithm) functions to describe them
- there are also many more

Gehrmann and Remiddi, hep-ph/0008287, hep-ph/0101124

For example,

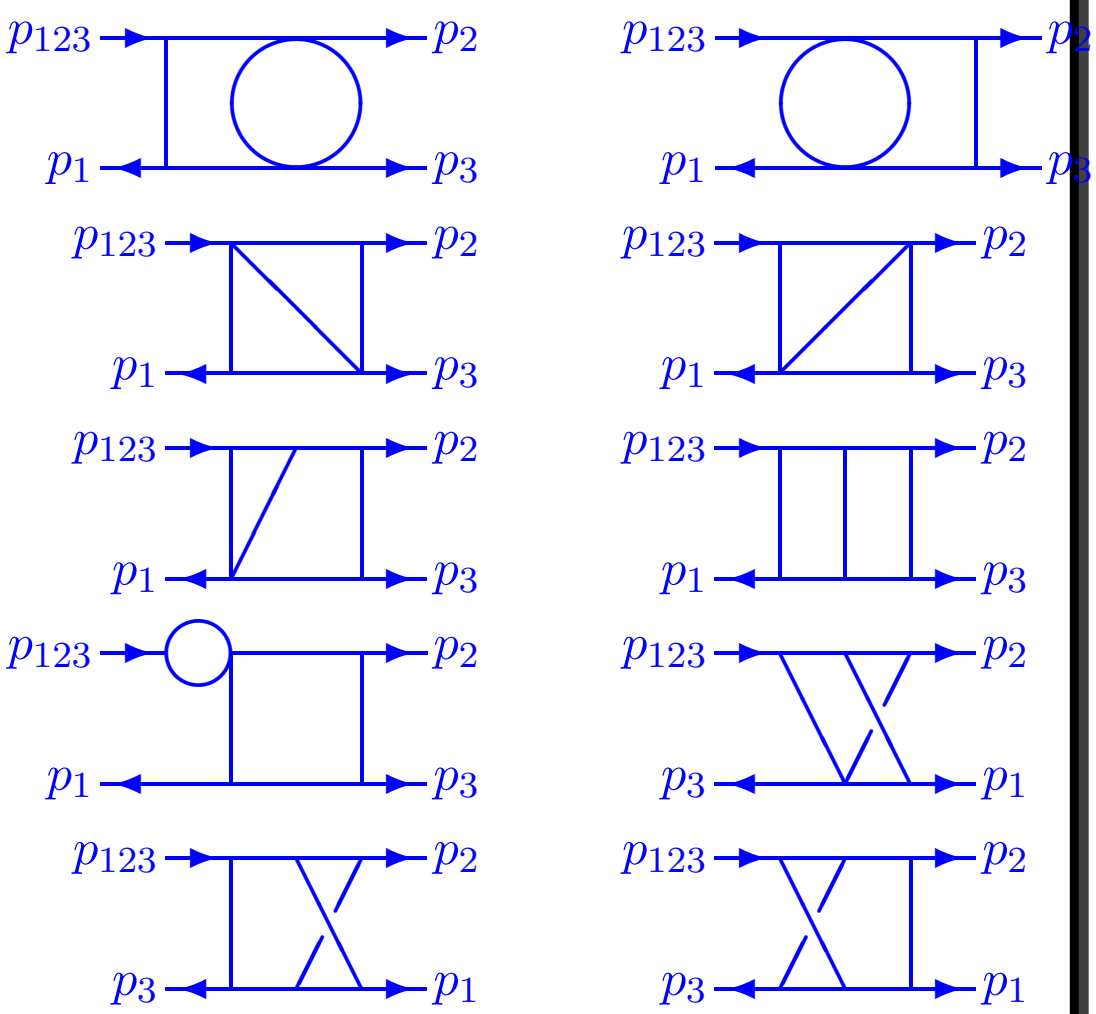

plus five extra integrals needed for the tensors.

Example of differential equation

Multiscale master integrals satisfy inhomogeneous differential equations in terms of invariants.

$$s_{123}\frac{\partial}{\partial s_{123}}$$ 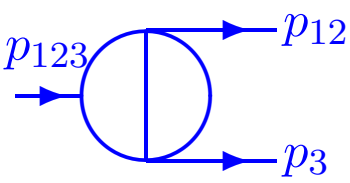

$$=$$

$$+\frac{d-4}{2}\,\frac{2s_{123}-s_{12}}{s_{123}-s_{12}}$$ 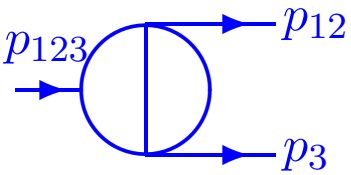

$$-\frac{3d-8}{2}\,\frac{1}{s_{123}-s_{12}}$$ 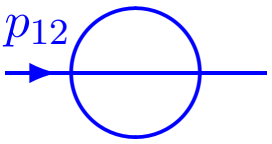

(1)

The boundary equations are in terms of simpler integrals.

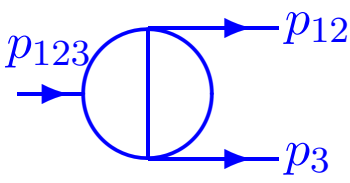

$$(s_{123}=0)=\frac{3d-8}{d-4}\,\frac{1}{s_{12}}$$ 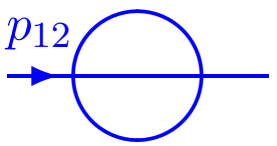

(2)

Example series expansion

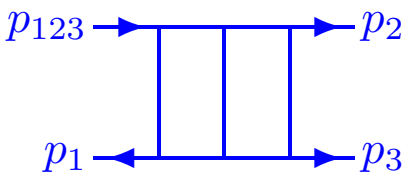

$$= \left(\frac{S_\epsilon}{16\pi^2}\right)^2 \frac{(-s_{123})^{-2\epsilon}}{s_{13}s_{23}^2} \sum_{i=0}^{4} \frac{f_{7.1,i}\left(\frac{s_{13}}{s_{123}}, \frac{s_{23}}{s_{123}}\right)}{\epsilon^i}$$

$$f_{7.1,4}(y,z) = -1 \ ,$$

$$f_{7.1,3}(y,z) = 2\left[H(0;y) + H(0;z)\right] \ ,$$

$$f_{7.1,2}(y,z) = -4H(0;y)H(0;z) - 4H(0,0;y) - 4H(0,0;z) - H(1,0;y) - 3H(1,0;z) - \frac{7\pi^2}{12} \ ,$$

$$\begin{aligned} f_{7.1,1}(y,z) = {} & +6H(0;y)H(1,0;z) + 2H(0;z)H(1-z,0;y) + 8H(0,0;y)H(0;z) \\ & +8H(0,0;z)H(0;y) + 8H(0,0,0;y) + 8H(0,0,0;z) + 5H(0,1,0;y) \\ & +6H(0,1,0;z) + 2H(1,0;z)H(1-z;y) + 2H(1,0,0;y) + 9H(1,0,0;z) \\ & -2H(1,1,0;y) + 6H(1,1,0;z) + 2H(1-z,1,0;y) - \frac{\zeta_3}{2} \\ & +\frac{\pi^2}{6}\left[+7H(0;y) + 7H(0;z) - 2H(1;y) + 6H(1;z) + 2H(1-z;y)\right] \ , \end{aligned}$$

$$\begin{aligned} f_{7.1,0}(y,z) = {} & -18H(0;y)H(1,0,0;z) - 12H(0;y)H(1,1,0;z) + 2H(0;z)H(1,1-z,0;y) \\ & -4H(0;z)H(1-z,0,0;y) - 2H(0;z)H(1-z,1-z,0;y) - 16H(0,0;y)H(0,0;z) \\ & -12H(0,0;y)H(1,0;z) + 2H(0,0;z)H(1,0;y) - 6H(0,0;z)H(1-z,0;y) \\ & -16H(0,0,0;y)H(0;z) - 16H(0,0,0;z)H(0;y) - 16H(0,0,0,0;y) \\ & -16H(0,0,0,0;z) - 16H(0,0,1,0;y) - 12H(0,0,1,0;z) - 12H(0,1,0;z)H(0;y) \\ & +2H(0,1,0;z)H(1;y) - 6H(0,1,0;z)H(1-z;y) - 10H(0,1,0,0;y) \\ & -18H(0,1,0,0;z) + H(0,1,1,0;y) - 12H(0,1,1,0;z) - 10H(0,1-z;y)H(1,0;z) \\ & -10H(0,1-z,0;y)H(0;z) - 10H(0,1-z,1,0;y) + 2H(1,0;y)H(1,0;z) \\ & +2H(1,0;z)H(1,1-z;y) - 4H(1,0;z)H(1-z,0;y) - 2H(1,0;z)H(1-z,1-z;y \\ & -6H(1,0,0;z)H(1-z;y) - 4H(1,0,0,0;y) - 21H(1,0,0,0;z) - 2H(1,0,1,0;y) \\ & -15H(1,0,1,0;z) + 2H(1,1,0;z)H(1;y) - 4H(1,1,0;z)H(1-z;y) \\ & +4H(1,1,0,0;y) - 21H(1,1,0,0;z) - 4H(1,1,1,0;y) - 12H(1,1,1,0;z) \\ & +2H(1,1-z,1,0;y) - 2H(1-z,0,1,0;y) - 4H(1-z,1,0,0;y) \\ & +4H(1-z,1,1,0;y) - 2H(1-z,1-z,1,0;y) - \frac{\pi^4}{4} \\ & +\zeta_3\left[+H(0;y) - 2H(1-z;y) - 6H(1;y) + 3H(1;z) + H(0;z)\right] \\ & +\frac{\pi^2}{6}\Big[- 14H(0;y)H(0;z) - 12H(0;y)H(1;z) + 2H(0;z)H(1;y) - 2H(0;z)H(1- \\ & -14H(0,0;y) - 14H(0,0;z) + H(0,1;y) - 12H(0,1;z) - 10H(0,1-z;y) \\ & +2H(1;y)H(1;z) - 4H(1;z)H(1-z;y) - 15H(1,0;z) - 4H(1,1;y) - 12H(1,1;z) \\ & +2H(1,1-z;y) - 4H(1-z,0;y) + 4H(1-z,1;y) - 2H(1-z,1-z;y)\Big] \ . \end{aligned}$$

Handling the thousands of integrals

• By projecting with (for example) tree-level, loop momenta always appear as nine possible dot-products

$$k.k,\ k.\ell,\ \ell.\ell,\ k.p_i,\ \ell.p_i,\quad i=1,\ldots,3$$

▷ These can always be written as nine possible propagators

$$(k+p_j)^2,\ (k-\ell)^2,\ldots$$

▷ Combine topologies into auxiliary loop integrals involving all nine possible propagators A_i

$$I^D_{t,r,s}(\{\nu_i\}) = \int \frac{d^Dk}{i\pi^{\frac{D}{2}}} \int \frac{d^D\ell}{i\pi^{\frac{D}{2}}} \frac{1}{A_1^{\nu_1}\ldots A_n^{\nu_n}}$$

where $\nu_i > 0$ if propagator appears in denominator
and $\nu_i \leq 0$ if it appears as an irreducible numerator

t counts number of different propagators
r counts total number of propagators
s counts number of loop momenta in the numerator

• Use 10 Integration-by-Parts (IBP) Kataev, Tkachov
and 3 Lorentz Invariance (LI) identities

Gehrmann, Remiddi hep-ph/9912329

to relate auxiliary integrals with different $\{\nu_i\}$

Calculational Strategy cont'd

- The IBP and LI identities relate integrals with more irreducible numerators (higher values of s), repeated propagators (higher r) and pinched propagators (smaller t)

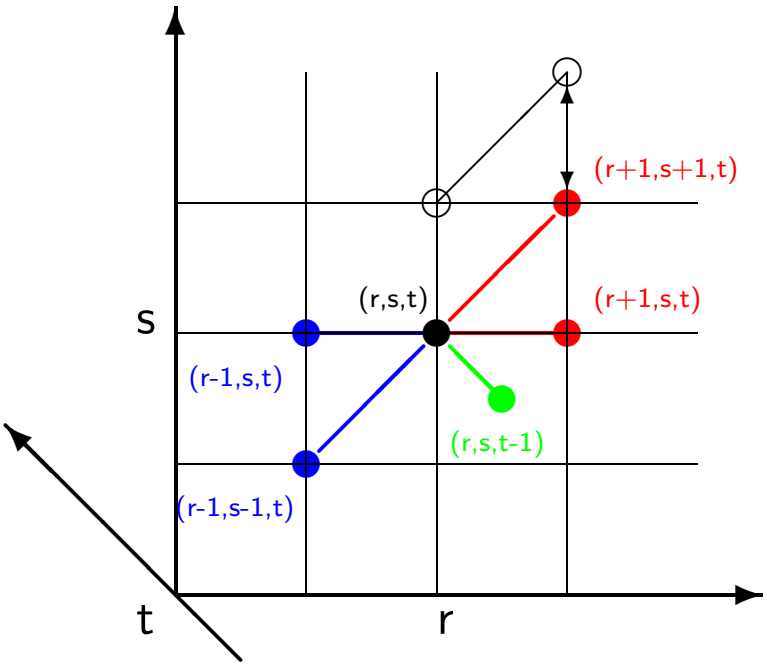

√ systematic procedure to reduce all possible auxiliary integrals to basis set of MI

√ to minimize the number of different topologies, introduce auxiliary diagrams - that, for example, describe *all* planar or non-planar topologies. Individual topologies are specific choices of the ν_i applied to the auxiliary integral.

Planar Auxiliary Diagram

- The general auxiliary planar diagram with propagator i raised to the power ν_i

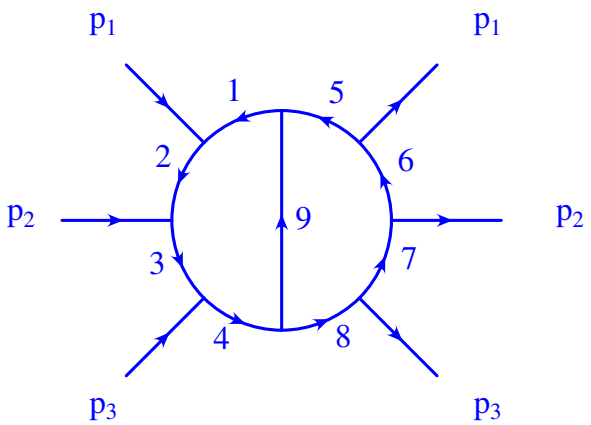

$$I^D(\nu_1, \nu_2, \nu_3, \nu_4, \nu_5, \nu_6, \nu_7, \nu_8, \nu_9)$$

$$\begin{aligned} A_1 &= k^2 & A_5 &= \ell^2 \\ A_2 &= (k+p_1)^2 & A_6 &= (\ell+p_1)^2 \\ A_3 &= (k+p_1+p_2)^2 & A_7 &= (\ell+p_1+p_2)^2 \\ A_4 &= (k+p_1+p_2+p_3)^2 & A_8 &= (\ell+p_1+p_2+p_3)^2 \\ A_9 &= (k-\ell)^2 \end{aligned}$$

e.g. the on-shell planar box integral

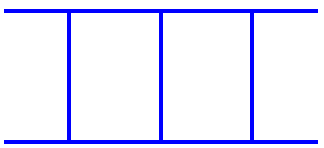

$$= I^D(1,1,1,0,1,0,1,1,1)$$

Planar IBP identities

$$
\begin{aligned}
s_{12}\nu_1 1^+ I^D &= -(D-\nu_1-\nu_2-2\nu_3-\nu_4-\nu_9)I^D \\
&\quad + \left((\nu_1 1^+ + \nu_2 2^+ + \nu_4 4^+)3^- + \nu_9 9^+(3^- - 7^-)\right) I^D, \\
\left(s_{23}\nu_2 2^+ + s_{123}\nu_1 1^+\right) I^D &= -(D-\nu_1-\nu_2-\nu_3-2\nu_4-\nu_9)I^D \\
&\quad + \left((\nu_1 1^+ + \nu_2 2^+ + \nu_3 3^+)4^- + \nu_9 9^+(4^- - 8^-)\right) I^D, \\
\left(s_{12}\nu_3 3^+ + s_{123}\nu_4 4^+\right) I^D &= -(D-2\nu_1-\nu_2-\nu_3-\nu_4-\nu_9)I^D \\
&\quad + \left((\nu_2 2^+ + \nu_3 3^+ + \nu_4 4^+)1^- + \nu_9 9^+(1^- - 5^-)\right) I^D, \\
s_{23}\nu_4 4^+ I^D &= -(D-\nu_1-2\nu_2-\nu_3-\nu_4-\nu_9)I^D \\
&\quad + \left((\nu_1 1^+ + \nu_3 3^+ + \nu_4 4^+)2^- + \nu_9 9^+(2^- - 6^-)\right) I^D, \\
s_{12}\nu_5 5^+ I^D &= -(D-\nu_5-\nu_6-2\nu_7-\nu_8-\nu_9)I^D \\
&\quad + \left((\nu_5 5^+ + \nu_6 6^+ + \nu_8 8^+)7^- + \nu_9 9^+(7^- - 3^-)\right) I^D, \\
\left(s_{23}\nu_6 6^+ + s_{123}\nu_5 5^+\right) I^D &= -(D-\nu_5-\nu_6-\nu_7-2\nu_8-\nu_9)I^D \\
&\quad + \left((\nu_5 5^+ + \nu_6 6^+ + \nu_7 7^+)8^- + \nu_9 9^+(8^- - 4^-)\right) I^D, \\
\left(s_{12}\nu_7 7^+ + s_{123}\nu_8 8^+\right) I^D &= -(D-2\nu_5-\nu_6-\nu_7-\nu_8-\nu_9)I^D \\
&\quad + \left((\nu_6 6^+ + \nu_7 7^+ + \nu_8 8^+)5^- + \nu_9 9^+(5^- - 1^-)\right) I^D, \\
s_{23}\nu_8 8^+ I^D &= -(D-\nu_5-2\nu_6-\nu_7-\nu_8-\nu_9)I^D \\
&\quad + \left((\nu_5 5^+ + \nu_7 7^+ + \nu_8 8^+)6^- + \nu_9 9^+(6^- - 2^-)\right) I^D,
\end{aligned}
$$

$$
\begin{aligned}
&(D-\nu_5-\nu_6-\nu_7-\nu_8-2\nu_9)I^D = \\
&\qquad \left(\nu_5 5^+(9^- - 1^-) + \nu_6 6^+(9^- - 2^-) + \nu_7 7^+(9^- - 3^-) + \nu_8 8^+(9^- - 4^-)\right) I^D, \\
&(D-\nu_1-\nu_2-\nu_3-\nu_4-2\nu_9)I^D = \\
&\qquad \left(\nu_1 1^+(9^- - 5^-) + \nu_2 2^+(9^- - 6^-) + \nu_3 3^+(9^- - 7^-) + \nu_4 4^+(9^- - 8^-)\right) I^D.
\end{aligned}
$$

I^D is a seed integral

$1^+(1^-)$ raises (lowers) the power of propagator 1.

These equations are enough for all planar topologies (on-shell and off-shell).

Planar Example

$I^D(1,0,0,1,0,1,1,0,1) =$ 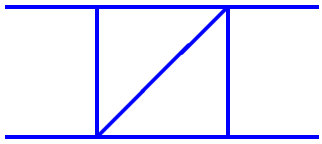 (s,t)

1 scalar master integral

+ 4 first rank tensor integrals (-1 in four positions)

+ 10 second rank integrals

+ 20 third rank integrals

+ 35 fourth rank integrals

$\Longrightarrow$ 69 integrals that may appear in a Feynman diagram calculation with upto four loop momenta in the numerator for this topology (with this momentum assignment)

• Automatically solve using a system of $69 \times 13 = 897$ equations by eliminating the unwanted integrals and writing the remaining integrals in terms of master integrals and simpler integrals with fewer propagators $\Longrightarrow$ MAPLE

$\surd$ Needs to be done once and for all for each topology

$\triangleright$ Other momentum assignments obtained using s/t symmetry and exchanging the two-loop momenta.

Equations and Unknowns

$t = 7$

\# different $I_{t,r,s}$

r \ s	0	1	2	3	4
7	1	2	3	4	5
8	7	14	21	28	35
9	28	56	84	112	140
10	84	168	252	336	420

accumulated \# equations
\# unknowns

r \ s	0	1	2	3
7	13 22	39 45	78 76	130 115
8	104 106	312 213	624 354	1040 535
9	468 358	1404 717	2808 1196	4680 1795

\# equations grows faster than \# unknowns so solution (always?) seems possible

On-shell Non-Planar Auxiliary Diagram

- The general auxiliary non-planar diagram with propagator i raised to the power ν_i

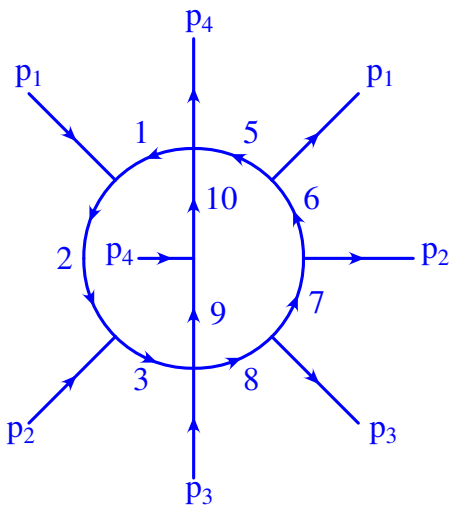

$$I^D(\nu_1, \nu_2, \nu_3, 0, \nu_5, \nu_6, \nu_7, \nu_8, \nu_9, \nu_{10})$$

where the $k.p_3$ now appears in the 10th propagator $(k-l-p_1-p_2-p_3)^2$ rather than the 4th propagator $(k+p_1+p_2+p_3)^2$

e.g. the on-shell nonplanar box integrals

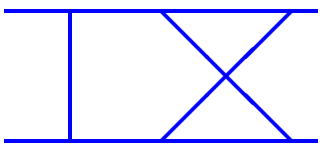

$$= \quad I^D(1,1,1,0,0,0,1,1,1,1)$$

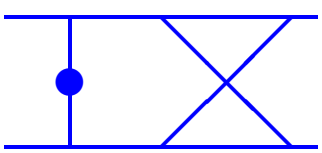

$$= \quad I^D(1,2,1,0,0,0,1,1,1,1)$$

- For non-planar off-shell diagrams, two auxiliary diagrams are needed

Matrix Element calculation

General algorithm

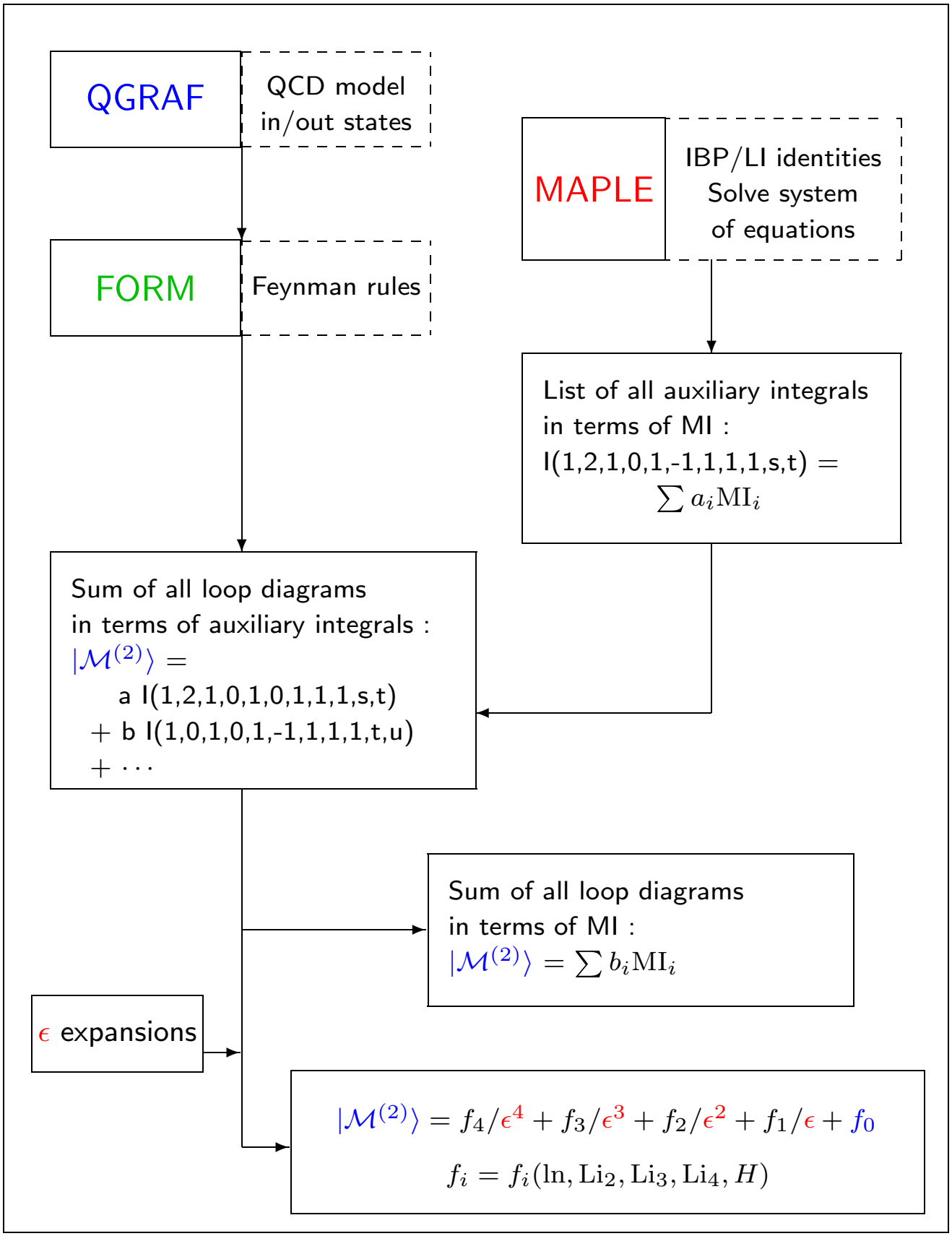

Helicity amplitudes or $\langle \mathcal{M}^{(0)} | \mathcal{M}^{(2)} \rangle$

- Projecting by the tree amplitude serves two purposes

  1) its what we need for NNLO calculations

  2) it saturates the Lorentz structure and puts the loop momenta in terms of the nine propagators

- Can just as easily extract the coefficients of the general tensor structure

e.g. $\gamma^* \to q(p_1)\bar{q}(p_2)g(p_3)$

$$\begin{aligned} \mathcal{S}_\mu(q;g;\bar{q}) &= + \sum_{I=1,2}\sum_{J=1,3} A_{IJ}(s_{13},s_{23},s_{123})T_{IJ\mu} \\ &+ B(s_{13},s_{23},s_{123})T_\mu, \end{aligned}$$

where A_{IJ} and B are gauge-independent functions and, for example, the non-vanishing tree-level structure is

$$\begin{aligned} T_\mu &= s_{23}\left(\bar{u}(p_1)\gamma_\mu u(p_2)\epsilon_3.p_1 + \frac{1}{2}\bar{u}(p_1)\not{\epsilon}_3\not{p}_3\gamma_\mu u(p_2)\right) \\ &- s_{13}\left(\bar{u}(p_1)\gamma_\mu u(p_2)\epsilon_3.p_2 + \frac{1}{2}\bar{u}(p_1)\gamma_\mu\not{p}_3\not{\epsilon}_3 u(p_2)\right). \end{aligned}$$

Helicity amplitudes or $\langle \mathcal{M}^{(0)} | \mathcal{M}^{(2)} \rangle$ cont.

▷ It is straightfoward to project out the general tensor coefficients, for example

$$\begin{aligned}\mathcal{P}(B) \quad = \quad & -\frac{1}{2(D-3)s_{12}^2 s_{13}^2} T_{11}^{\dagger\mu} - \frac{(D-2)}{2(D-4)s_{12}^2 s_{13} s_{23}(D-3)} T_{12}^{\dagger\mu} \\ & + \frac{1}{2s_{23}s_{12}(D-3)s_{13}^2} T_{13}^{\dagger\mu} + \frac{(D-2)}{2(D-4)s_{12}^2 s_{13} s_{23}(D-3)} T_{21}^{\dagger\mu} \\ & + \frac{1}{2s_{23}^2 s_{12}^2 (D-3)} T_{22}^{\dagger\mu} - \frac{1}{2s_{13}s_{12}(D-3)s_{23}^2} T_{23}^{\dagger\mu} \\ & + \frac{1}{2(D-4)s_{12}^2 s_{13} s_{23}} T^{\dagger\mu}\end{aligned}$$

isolates the tensor coefficient B.

▷ Valid at all orders in perturbation theory..

▷ The action of the projector is to make all quantities Lorentz scalars, and in our applications means we can access the IBP/LI identities for the auxiliary diagrams directly

Helicity amplitudes or $\langle \mathcal{M}^{(0)} | \mathcal{M}^{(2)} \rangle$ cont.

▷ It is a separate exercise to relate the tensor coefficients to the helicity amplitudes or to recove the interference of tree and loop amplitudes

For example,

$$\mathcal{S}_{\dot{A}B}(q+;g+;\overline{q}-) =$$
$$+\alpha\,\frac{p_{1\dot{A}D}p_2^D p_{2B}}{\langle p_1 p_3\rangle\langle p_3 p_2\rangle} + \beta\,\frac{p_{3\dot{A}D}p_2^D p_{2B}}{\langle p_1 p_3\rangle\langle p_3 p_2\rangle} + \gamma\,\frac{p_{1\dot{C}B}p_3^{\dot{C}} p_{3\dot{A}}}{\langle p_1 p_3\rangle\langle p_3 p_2\rangle^*}$$
$$+\,\delta\,\frac{\langle p_1 p_3\rangle^*}{\langle p_1 p_3\rangle\langle p_1 p_2\rangle^*}\left(p_{1\dot{A}B}+p_{2\dot{A}B}+p_{3\dot{A}B}\right)\ .$$

where

$$\begin{aligned}
\alpha &= \frac{s_{23}s_{13}}{4}\Big(2B + A_{12} - A_{11}\Big),\\
\beta &= \frac{s_{13}}{4}\Big(2s_{23}B + 2(s_{12}+s_{13})A_{11} + s_{23}\big(A_{12}+A_{13}\big)\Big),\\
\gamma &= \frac{s_{13}s_{23}}{4}\Big(A_{11} - A_{13}\Big),\\
\delta &= -\frac{s_{12}s_{13}}{4}A_{11}.
\end{aligned}$$

Checks of results

- Infrared singularity structure Catani, hep-ph/9802439

$$|\mathcal{M}^{(2)}\rangle = \boldsymbol{I}^{(1)}(\epsilon)\,|\mathcal{M}^{(1)}\rangle + \boldsymbol{I}^{(2)}(\epsilon)\,|\mathcal{M}^{(0)}\rangle + |\mathcal{M}^{(2)\,\mathrm{fin}}\rangle$$

▷ first term: the process dependent but predictable one-loop insertion operator $\boldsymbol{I}^{(1)}$ acts onto one-loop matrix element

▷ second term: new colour-charge operator $\boldsymbol{I}^{(2)}$ acts onto tree-level matrix element,

$$\begin{aligned}\boldsymbol{I}^{(2)}(\epsilon) \;=\; & -\frac{1}{2}\boldsymbol{I}^{(1)}(\epsilon)\left(\boldsymbol{I}^{(1)}(\epsilon)+\frac{2\beta_0}{\epsilon}\right) \\ & +e^{-\epsilon\gamma}\frac{\Gamma(1-2\epsilon)}{\Gamma(1-\epsilon)}\left(\frac{\beta_0}{\epsilon}+K\right)\boldsymbol{I}^{(1)}(2\epsilon)+\boldsymbol{H}^{(2)}\end{aligned}$$

▷ The function $\boldsymbol{H}^{(2)}$ contains only single poles and is process and scheme dependent.

- High energy limit :

in the $t \to 0$ limit, the parton-parton scattering amplitudes should reproduce the $\log(-s/t)$ structure resummed by the BFKL equation.

Infrared singularity structure cont

Catani, hep-ph/9802439

- pole structure of two-loop amplitude interfered with tree-level

$$\begin{aligned}\mathcal{P}oles = 2\,\mathrm{Re}\Bigg[& \frac{1}{2}\langle\mathcal{M}^{(0)}|\boldsymbol{I}^{(1)}(\epsilon)\boldsymbol{I}^{(1)}(\epsilon)|\mathcal{M}^{(0)}\rangle \\ & + \langle\mathcal{M}^{(0)}|\boldsymbol{I}^{(1)}(\epsilon)|\mathcal{M}^{(1)\,fin}\rangle - \frac{\beta_0}{\epsilon}\,\langle\mathcal{M}^{(0)}|\boldsymbol{I}^{(1)}(\epsilon)|\mathcal{M}^{(0)}\rangle \\ & + e^{-\epsilon\gamma}\,\frac{\Gamma(1-2\epsilon)}{\Gamma(1-\epsilon)}\left(\frac{\beta_0}{\epsilon}+K\right)\langle\mathcal{M}^{(0)}|\boldsymbol{I}^{(1)}(2\epsilon)|\mathcal{M}^{(0)}\rangle \\ & + \langle\mathcal{M}^{(0)}|\boldsymbol{H}^{(2)}(\epsilon)|\mathcal{M}^{(0)}\rangle\Bigg]\end{aligned}$$

- The finite remainder is defined as

$$\mathcal{F}inite = 2\,\mathrm{Re}\langle\mathcal{M}^{(0)}|\mathcal{M}^{(2)}\rangle - \mathcal{P}oles$$

and is typically given in terms of real logs and polylogs for each scattering channel and each colour

Infrared pole structure

The singularity structure is due to factorisation of the amplitude

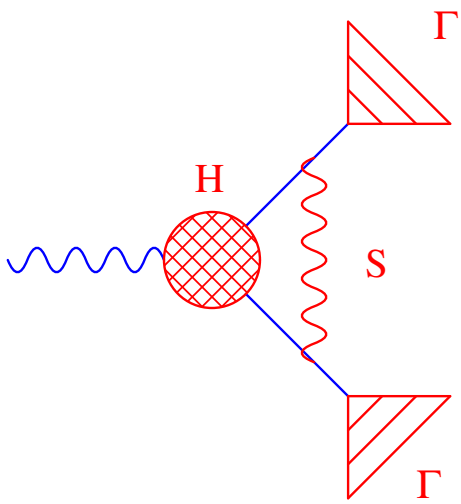

$$\mathcal{M} = H\Gamma^2 S$$

where

- H is the hard scattering
- Γ is collinear intrajet radiation - resummed by exponentiated Sudakov factor
- S is soft interjet radiation - including all colour correlations between the hard partons - resummed by exponentiated soft anomalous dimension

reproduces exactly the singular structure (including colour correlations of H_2) Sterman and Tejeda-Yeomans

Finite parts

e.g., leading colour part of $q_1\bar{q}_1 \longrightarrow q_2\bar{q}_2$

$$
\begin{aligned}
A_s \quad = \quad & \left[2\,\mathrm{Li}_4(x) + \left(-2\,X - \frac{11}{3} \right) \mathrm{Li}_3(x) + \left(X^2 + \frac{11}{3}\,X - \frac{2}{3}\,\pi^2 \right) \mathrm{Li}_2(x) \right. \\
& + \frac{121}{18}\,S^2 + \left(-\frac{11}{3}\,X^2 + 11\,X - \frac{296}{27} \right) S + \frac{1}{6}\,X^4 + \left(\frac{1}{3}\,Y - \frac{49}{18} \right) X^3 \\
& + \left(\frac{11}{6}\,Y - \frac{5}{6}\,\pi^2 + \frac{197}{18} \right) X^2 + \left(-\frac{2}{3}\,Y\,\pi^2 - \frac{47}{18}\,\pi^2 + 6\,\zeta_3 - \frac{95}{24} \right) X \\
& \left. + \left(\frac{11}{24}\,\pi^2 - 7\,\zeta_3 - \frac{409}{216} \right) Y + \frac{113}{720}\,\pi^4 - \frac{7}{6}\,\pi^2 + \frac{197}{36}\,\zeta_3 + \frac{23213}{2592} \right] \left[\frac{t^2+u^2}{s^2} \right] \\
& + \left[-3\,\mathrm{Li}_4(y) + 6\,\mathrm{Li}_4(x) - 3\,\mathrm{Li}_4(z) + \left(-2\,X - \frac{7}{2} \right) \mathrm{Li}_3(x) \right. \\
& + 3\,X\,\mathrm{Li}_3(y) + \left(\frac{1}{2}\,X^2 + \frac{7}{2}\,X + \frac{1}{2}\,\pi^2 \right) \mathrm{Li}_2(x) + \left(-\frac{11}{6}\,X^2 + \frac{11}{6}\,X \right) S \\
& + \left(\frac{1}{2}\,Y\,\pi^2 - \frac{13}{9}\,\pi^2 - \zeta_3 - \frac{32}{9} \right) X + \left(\frac{7}{4}\,Y - \frac{3}{4}\,\pi^2 + \frac{44}{9} \right) X^2 \\
& \left. + \left(\frac{1}{2}\,Y - \frac{49}{36} \right) X^3 - \frac{7}{120}\,\pi^4 + \frac{47}{36}\,\pi^2 + 2\,\zeta_3 \right] \left[\frac{t^2-u^2}{s^2} \right] + \left[3\,X^2 \right] \frac{t^3}{s^2 u} \\
& + 3\,\mathrm{Li}_4(y) - 3\,\mathrm{Li}_4(x) + 3\,\mathrm{Li}_4(z) - 3\,X\,\mathrm{Li}_3(y) - \frac{5}{2}\,\mathrm{Li}_3(x) \\
& + \left(\frac{5}{2}\,X - \frac{1}{2}\,\pi^2 \right) \mathrm{Li}_2(x) - \frac{11}{6}\,X\,S + \frac{1}{8}\,X^4 + \left(-\frac{1}{2}\,Y + \frac{1}{3} \right) X^3 \\
& + \left(\frac{5}{4}\,Y + \frac{1}{4}\,\pi^2 + \frac{1}{6} \right) X^2 + \left(-\frac{1}{2}\,Y\,\pi^2 - \frac{7}{6}\,\pi^2 + 3\,\zeta_3 + \frac{32}{9} \right) X \\
& + \frac{1}{40}\,\pi^4 - \frac{11}{36}\,\pi^2 + 4\,\zeta_3
\end{aligned}
$$

$$x = -\frac{t}{s}, \quad y = -\frac{u}{s}, \quad X = \ln(x), \quad Y = \ln(y), \quad S = \ln\left(\frac{s}{\mu^2}\right)$$

High Energy Limit

Del Duca, NG, hep-ph/0109028

- In the high energy limit, the scattering amplitude has the factorised form in terms of impact factors and reggeized gluon exchange

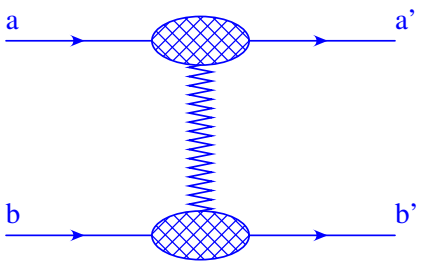

  which sums the leading and next-to-leading logs of $-s/t$.

▷ Expanding the impact factors and the gluon regge trajectory and comparing with the $t \to 0$ limit of the explicit two-loop matrix element calculation

- check the (leading) double logarithmic term

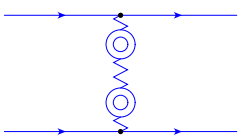

- check the (next-to-leading) single logarithm

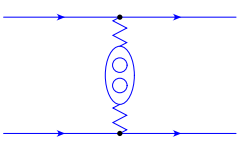
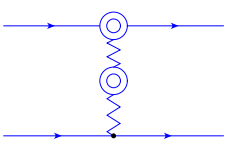
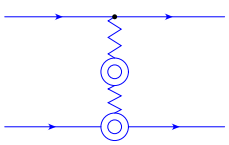

  in terms of the leading trajectory and the one-loop impact factors and the next-to-leading trajectory

High Energy Limit cont'd

√ Universal behaviour of the factorized scattering ansätz

√ Confirm the next-to-leading virtual corrections to the gluon regge trajectory

Fadin, Fiore and Kotsky, Phys. Lett. B359, (1995) 181

Fadin, Fiore and Kotsky, hep-ph/9605357

Fadin, Fiore and Quartarolo, hep-ph/9506432

Blümlein, Ravindran and ven Neerven, hep-ph/9806357

X See that scattering ansätz breaks down at the next-to-next-to-leading log level i.e. constant

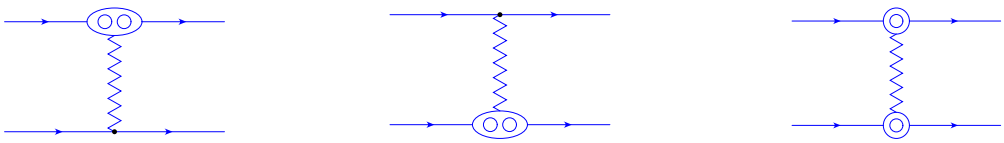

through violation of the relation between next-to-next-leading order impact factors

— not unexpected, and probably due to exchange of other colour structures

√ Also find the next-to-leading virtual corrections to the quark regge trajectory Bogdan, Del Duca, Fadin + NG, hep-ph/0201240

Progress in NNLO QCD - Conclusions

- ▷ NNLO QCD calculations for scattering processes are required for theoretical predictions to challenge the high statistics experimental data from LEP, HERA, TEVATRON, LHC and LC...
- ▷ The bottleneck has been calculating the two-loop box graphs, which form a crucial part of the NNLO predictions for jet cross sections. However there has been enormous progress in the last two years
- ▷ Many $2 \to 2$ scattering processes with up to one off-shell leg now calculated at two-loops
  - $\surd$ strong checks with infrared pole structure, high energy limit, QED results
  - $\surd$ must be combined with the tree-level $2 \to 4$, the one-loop $2 \to 3$ and the self-interference of the one-loop $2 \to 2$ to yield physical cross sections
  - — this is still some way away but lots of ideas and expect first NNLO parton level Monte Carlos in next couple of years.
- ▷ Together with NNLO DIS, Drell-Yan and the exact calculations of the splitting functions, the NNLO $pp \to$jet+X cross section will make form a global set of NNLO variables that can test QCD over a wide range of energies